Geochemical Perspectives Letters

Spinodal decomposition of supercritical fluid forms melt network in a silicate-H_2O system

Q.X. Wang, D.Y. Zhou, W.-C. Li, H.W. Ni

Supplementary Information

The Supplementary Information includes:

- Materials and Methods
- Table S-1
- Figures S-1 and S-2
- Videos S-1 to S-8
- Supplementary Information References

Materials and Methods

Starting material

Anhydrous $Na_3AlSi_5O_{13}$ glass was prepared from fusing reagent-grade oxides and carbonates at 1200 °C for 24 h followed by quench in water. Hydrous glass was synthesised by sealing distilled water and anhydrous glass powder into a Pt capsule and annealing at 1000 °C and 1 GPa for 24 h in a piston-cylinder apparatus. Water content was determined to be 1.5 wt. % by a PerkinElmer Spotlight 200 microscope attached to a Frontier Fourier-transform infrared spectrometer. Doubly polished hydrous glass sections with a thickness of ~80 μm were prepared for hydrothermal diamond anvil cell (HDAC) experiments.

Hydrothermal diamond anvil cell setup

An externally heated Bassett-type hydrothermal diamond anvil cell (HDAC; Bassett *et al*., 1993) equipped with two type IIa diamonds with a culet size of 1 mm was used in our experiments. Rhenium gasket with an initial thickness of 125 μm and a 400 μm (500 μm for Run#306 and Run#307) pinhole was used to accommodate the sample. Heating was provided by two Pt wire heaters, and temperature was monitored by two type-K thermocouples in direct contact with the diamonds. Because the sample chamber after several cycles of heating and cooling behaved nearly isochoric (Bassett *et al*., 1993), the pressure at a given temperature can be inferred from total fluid density and the equation of state of H_2O (Wagner and Pruß, 2002). This calculation implies small or negligible excess volumes of mixing when water dissolves in the silicate melt or the silicate dissolves in the aqueous fluid. The pressure in one experiment (Run#306) was also estimated by using the Raman shift of zircon band at 1008 cm^{-1} (Schmidt *et al*., 2013). Emission

lines of a Ne lamp were used to calibrate the wavenumber. The uncertainty of pressure estimated from zircon is ±0.05 GPa (Schmidt *et al*. 2013). Comparison between the zircon barometer and calculation base on the equation of state of H_2O indicates that the uncertainty in our pressure estimates is probably of the order of ±0.1 GPa (Fig. S-1).

Calculation of silicate to H_2O mass ratio

The silicate to H_2O mass ratio of each experiment is presented in Table S-1. Before each experiment (except for Run#104), the volume of the cell (sample chamber) was determined with vapour-saturated water only. According to Audétat and Keppler (2005), cell volume (V_{cell}) can be estimated from the size of vapour bubble at a given temperature (V_{vap}), the corresponding densities of vapour and liquid (ρ_{vap} and ρ_{liq}), and the total density of the sample chamber (ρ_{tot}, inferred from vapour-liquid homogenisation temperature) using the following relationship:

$$V_{cell} = \frac{V_{vap} \cdot (\rho_{vap} - \rho_{liq})}{\rho_{tot} - \rho_{liq}} \qquad \text{(Eq. S-1)}$$

In each experiment, V_{vap} was measured at least at five different temperatures for computation of V_{cell}.

In phase separation experiments, the approach above was also used to calculate the fluid accessible volume (*i.e.* excluding the volume of glass) whenever applicable. The total fluid density (also excluding glass) was derived from the homogenisation temperature of water and vapour bubble. The product of fluid accessible volume and total fluid density gives the mass of water. In a few experiments for which the approach above was not applicable, the fluid accessible volume was calculated as the difference between V_{cell} and the volume of glass wafer (see below), and the total fluid density was taken as 1.0 g/cm^3.

The area of silicate glass wafer (A) was measured by optical microscopy (Carl Zeiss Axio Scope.A1). Wafer thickness (h) was measured by a micrometre. Glass density (ρ_{gl}) was estimated to be 2.4 g/cm^3 according to Bagdassarov et al. (2000). The mass of glass wafer is calculated as S. The overall uncertainty of the calculated silicate to H_2O mass ratio is estimated to be ±10 % relative.

***In situ* Raman spectroscopy**

Raman spectra were collected on supercritical fluid, hydrothermal fluid and silicate melt with a Horiba Jobin-Yvon LabRam HR Evolution spectrometer. The acquisition setup involved a 532 nm Nd:YAG laser of 500 mW output power (~55 mW at the sample), a confocal hole of 400 μm diameter, a slit of 100 μm width, an objective of 20 × magnification (numerical aperture = 0.25), a spectral range of 200–4200 cm^{-1} with 600 grooves/mm grating, and a CCD detector (1024 × 256 pixels of 26 × 26 μm). Acquisition time was typically 4 min per spectrum (2 accumulations of 15 s per spectral window).

Supplementary Table

Table S-1 Details of phase separation experiments.

Run	Silicate glass		Water				Silicate to H_2O ratio	Silicate content wt. %	Phase separation mechanism[b]
	volume 10^{-12} m^3	mass µg	V_{liq1}[a] 10^{-12} m^3	V_{liq2}[a] 10^{-12} m^3	density g/cm^3	mass µg			
819[c]	2.84	6.8	14.4		~1.0	14.4	0.47	32	NG
821_1[c]	2.75	6.6	13.2		~1.0	13.2	0.50	33	NG
627_1	3.10	7.4	14.5	14.9	0.985	14.2	0.52	34	NG
104[c]	3.28	7.9	14.9		~1.0	14.9	0.53	35	NG
306	4.59	11.0	19.8	21.8	0.956	20.8	0.53	35	NG
623	3.37	8.1	15.1	15.2	0.984	14.9	0.54	35	SD-D
818[c]	3.16	7.6	14.1		~1.0	14.1	0.54	35	SD-D
626	3.22	7.7	14.0	14.7	0.987	13.8	0.56	36	SD-D/N
622	3.34	8.0	14.4	14.6	0.984	14.2	0.57	36	SD-D
705	3.45	8.3	14.6	13.9	0.987	14.4	0.57	36	SD-D
625	3.31	8.0	13.9	14.7	0.986	13.7	0.58	37	SD-N
621	3.55	8.5	14.4	14.5	0.988	14.2	0.60	38	SD-N
624_2	3.62	8.7	14.4	14.4	0.986	14.2	0.61	38	SD-N
620	3.65	8.8	13.8	14.3	0.977	13.5	0.65	39	SD-N
708	3.63	8.7	14.0	13.7	0.984	13.8	0.63	39	SD-N
527	3.50	8.4	13.4	11.5	0.992	12.4[d]	0.68	40	SD-N
619	3.79	9.1	13.2	13.6	0.974	12.9	0.71	41	SD-N
624_1	4.03	9.7	13.0	14.0	0.991	13.3[d]	0.73	42	SD-N
603_1	3.80	9.1	12.2	11.3	0.988	11.6[d]	0.78	44	SD-N
821_2[c]	4.07	9.8	11.9		~1.0	11.9	0.82	45	SD-N
307[c]	6.50	15.60	16.9		~1.0	16.9	0.92	48	SD-N
629	5.33	12.8	13.6	11.2	0.981	12.5[d]	1.02	51	SD-N
603_2	5.31	12.7	14.7	9.7	0.990	12.1[d]	1.05	51	SD-N
627_2	7.63	18.3	12.5	9.6	0.982	10.8[d]	1.69	63	SD-D

[a] V_{liq1} is the fluid accessible volume calculated from the volume difference between the cell and the glass, and V_{liq2} is the fluid accessible volume directly measured with the aid of a vapour bubble. The latter value is adopted whenever applicable.

[b] NG, nucleation-growth; SD-D, spinodal decomposition forming droplets; SD-N, spinodal decomposition forming a silicate melt network.

[c] Vapour bubble vanished quickly after heating, which prohibits accurate determination of V_{liq2} and fluid density.

[d] Calculated using a fluid accessible volume as the average of V_{liq1} and V_{liq2} due to the large difference between them.

Supplementary Figures

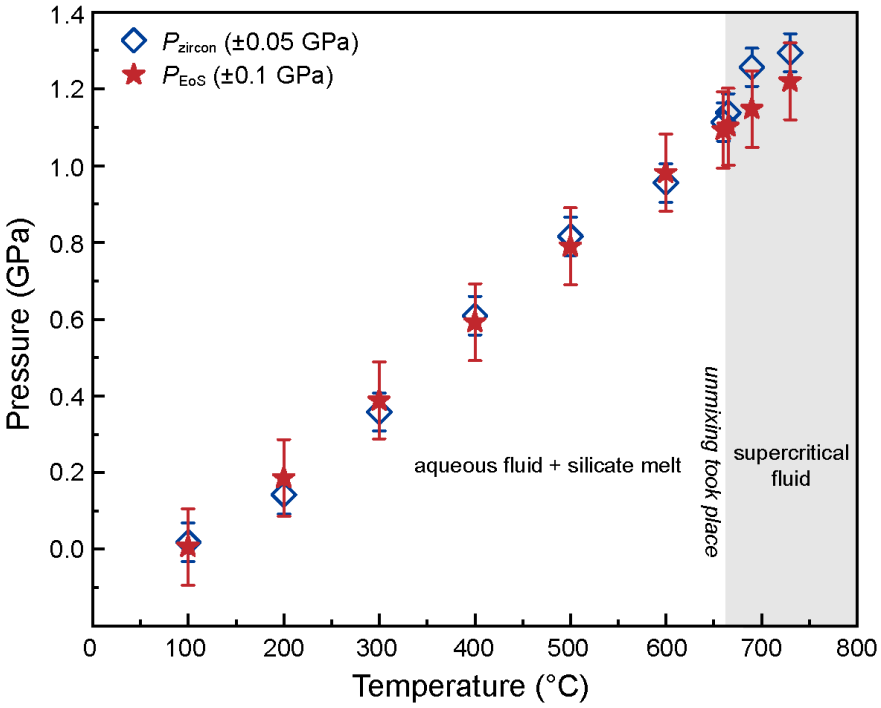

Figure S-1 Variations of pressure with temperature in Run#306, as estimated from the Raman shift of zircon band at ~1008 cm^{-1} (blue diamonds, P_{zircon}; Schmidt *et al*., 2013) and from the EoS of water (red stars, P_{EoS}; Wagner and Pruß, 2002). The uncertainties are ±0.05 GPa for P_{zircon} and ±0.1 GPa for P_{EoS}. Unmixing of supercritical fluid with S/H of 0.53 took place at 664 °C by nucleation-growth.

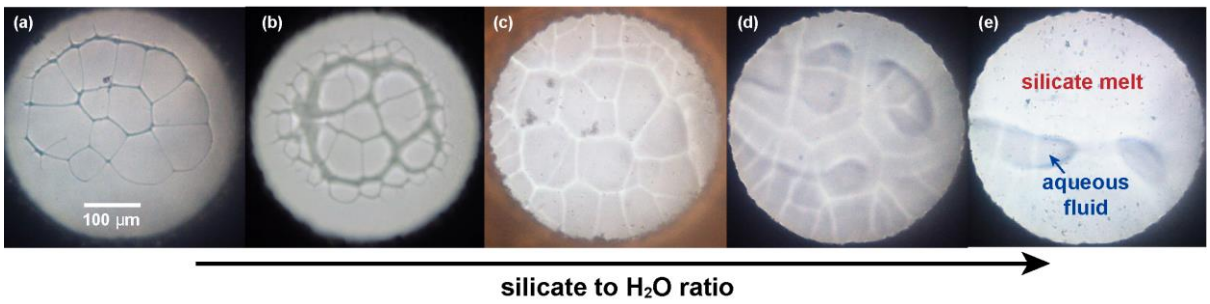

Figure S-2 Silicate to H_2O ratios (by mass) from **(a)** to **(e)** are 0.58, 0.68, 0.73, 1.02 and 1.69, respectively. The network of silicate melt quickly collapsed into melt droplets in **(a)**–**(d)**, whereas the large portions of melt and fluid in **(e)** persisted for long time. The different contrast of images [*i.e.* melt being dark in **(a)** and **(b)** but bright in **(c)**, **(d)** and **(e)**] was due to different focus.

Supplementary Videos

Videos of typical phase separation processes of supercritical fluid

(caption: silicate to H_2O ratio_run number_phase separation mechanism)

Video S-1 0.53_104_NG
Video S-2 0.56_626_SD-DN
Video S-3 0.57_705_SD-D
Video S-4 0.58_625_SD-N
Video S-5 0.63_708_SD-N
Video S-6 0.68_527_SD-N
Video S-7 0.78_603_SD-N
Video S-8 1.69_627_SD-D

The video files are available for download (.GIF files) at https://www.geochemicalperspectivesletters.org/article2119.

Supplementary Information References

Audétat, A., Keppler, H. (2005) Solubility of rutile in subduction zone fluids, as determined by experiments in the hydrothermal diamond anvil cell. *Earth and Planetary Science Letters* 232, 393–402.

Bagdassarov, N., Dorfman, A., Dingwell, D.B. (2000) Effect of alkalis, phosphorus, and water on the surface tension of haplogranite melt. *American Mineralogist* 85, 33–40.

Bassett, W.A., Shen, A.H., Bucknum, M., Chou, I.M. (1993) A new diamond anvil cell for hydrothermal studies to 2.5 GPa and from −190 °C to 1200 °C. *Reviews of Scientific Instruments* 64, 2340–2345.

Schmidt, C., Steele-MacInnis, M., Watenphul, A., Wilke, M. (2013) Calibration of zircon as a Raman spectroscopic pressure sensor to high temperatures and application to water-silicate melt systems. *American Mineralogist* 98, 643–650.

Wagner, W., Pruß, A. (2002) The IAPWS formulation 1995 for the thermodynamic properties of ordinary water substance for general and scientific use. *Journal of Physical and Chemical Reference Data* 31, 387–535.